

MIM capacitors are used for dc blocking and bypass. Via holes are provided for rf and dc grounding. Two shunt MIM capacitors and a resistor compose the bypass circuitry. The smaller capacitor directly bypasses rf signals at the operation frequencies while a larger one following the resistor bypasses signals at lower frequencies.

The resistor acts as a damping element to suppress excess out-of-band gain and stabilize the amplifier, because InP HEMT devices inherently have high gain at low frequencies. In addition, the resistor can de-Q the bypass circuitry to eliminate unwanted resonances caused by shunt capacitors and via-hole parasitic inductance.

III. MEASUREMENT

Figure 2 shows a photograph of the Ka-band three-stage MMIC LNA. The chip occupies an area of 1.7 mm^2 which measures 2.1 mm by 0.82 mm. The chips were first tested on-wafer using an Anritsu 37397C vector network analyzer (VNA). Input and output signals were coupled through ground-signal-ground (GSG) probes while dc voltages were supplied via a dc probe card. A short-open-load-through (SOLT) calibration was performed with a GGB CS-5 calibration substrate, placing the reference plane at the probe tips. The measurement was made at $V_D = 0.7 \text{ V}$ and a total current of 20.0 mA, corresponding to a dc power consumption of 14 mW. The measured s-parameters at Ka-band frequencies are shown in Fig. 3. From 26 GHz to 40 GHz, the amplifier achieves 25.0-dB gain with 1.9-dB flatness. The flatness of the amplifier is defined by

$$\text{Flatness (dB)} = (\text{Gain,max} - \text{Gain,min}) / 2 \quad (1)$$

Both input and output return loss are better than 10.0 dB across the entire Ka-band. Near the center of the band at 34 GHz, the gain is 26 dB with return loss better than 20.0 dB. Well-matched ports can eliminate the need for off-chip matching networks and thereby reduce system complexity. Fig. 4 shows the results from 0.5 GHz to 65 GHz. Within this frequency range, the K factor is greater than 1 assuring unconditional stability.

The noise performance was characterized by the Y-factor method using an Agilent N8975A noise figure meter (NFM) with a 12-dB excess noise ratio (ENR) noise diode (HP R347B). The noise diode was followed by a 6-dB attenuator to improve the difference in source impedance between on- and off-states and to reduce ENR as well. The N8975A can only detect signals below 26 GHz. Thus, a mixer (Spacek Labs Rka-14) was used to convert Ka-band signals down to 30MHz. Noise figure at room temperature (290K) was measured as the amplifier was biased for minimum noise figure at $V_D = 0.8 \text{ V}$ and a total current of 20.0 mA.

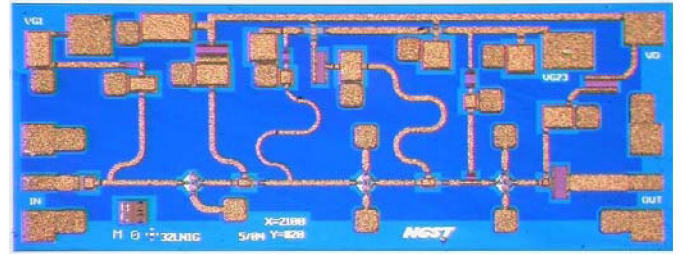


Fig. 2. Photograph of Ka-band MMIC LNA. The compact die measures 2.1 mm by 0.82 mm with a thickness of 75 μm .

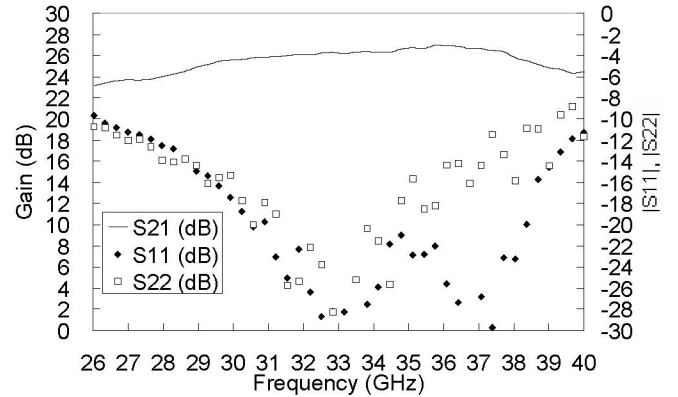


Fig. 3. Measured s-parameters at Ka-band frequencies.

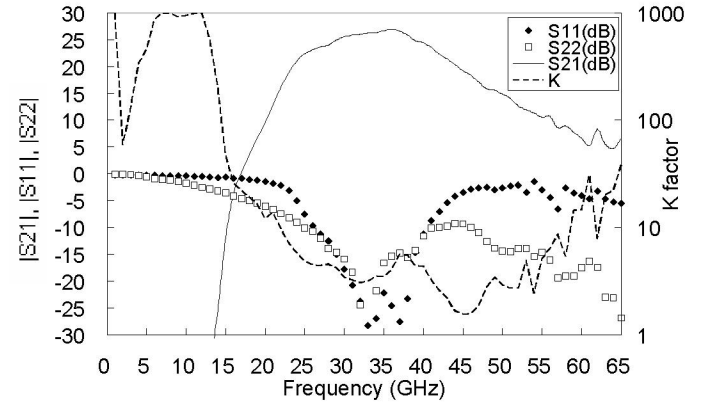


Fig. 4. Measured s-parameters from 0.5 GHz to 60 GHz.

Thus, a mixer (Spacek Labs Rka-14) was used to convert Ka-band signals down to IF. Noise figure at room temperature (290K) was measured as the amplifier was biased for minimum noise figure at $V_D = 0.8 \text{ V}$ and a total current of 20.0 mA. Figure 5 shows the measured noise temperature and associated gain. From 26 GHz to 40 GHz, the average noise temperature is 123.5 K, corresponding to 1.5 dB noise figure. Noise temperature is converted into noise figure by using

$$\text{Noise Figure (dB)} = 10 \log \left[1 + \frac{\text{Noise Temp}}{290} \right] \quad (2)$$

The associated gain is 21.9 dB with 0.9-dB flatness. Noise figure reaches a minimum of 1.3 dB at 34 GHz with

associated gain of 22.5 dB. Overall in Ka-band, the noise figure is below 1.9 dB and associated gain higher than 21.0 dB. The slight ripple in measured noise temperature is due to mismatch between waveguide components in the test setup. Mismatch could be reduced with the addition of an isolator or attenuator.

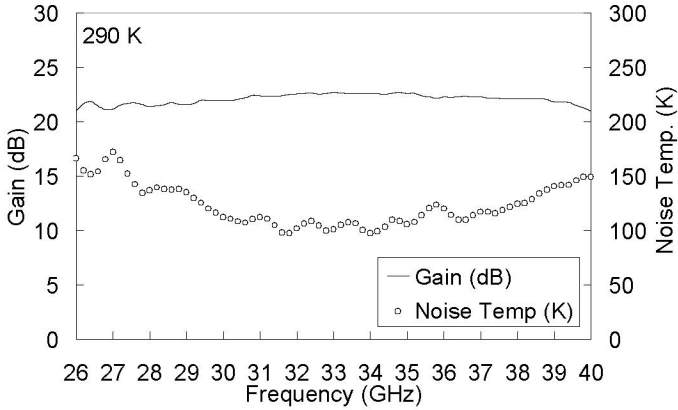


Fig. 5. Measured noise temperature and associated gain of the MMIC LNA, from 26 GHz to 40 GHz, at 290 K.

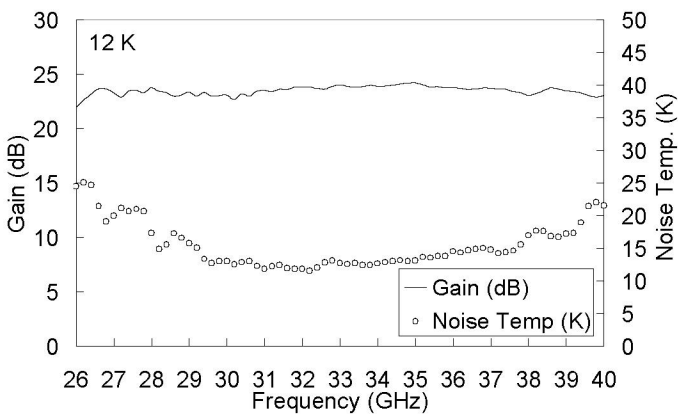


Fig. 6. Measured noise temperature and associated gain of the MMIC LNA, from 26 GHz to 40 GHz, at 12 K.

The noise performance was then measured with the amplifier operating cryogenically. As shown in Fig. 6, the noise temperature can be greatly reduced to an average of 15.5 K by cooling the amplifier down to an ambient temperature of 12 K and adjusting the bias to $V_D = 0.7$ V with a total current of 8.5 mA. The associated gain is 23.0 dB with 1.1-dB flatness. The minimum noise figure occurs at the center of the band. At 34 GHz, noise temperature reaches a minimum of 11.8 K, equivalent to a noise figure of 0.17 dB using (2).

IV. KA-BAND LNA MODULE

For a system that calls for higher gain, a multi-chip module is required. Such high gain would be difficult to achieve in a single chip, as well as being risky in terms of stability, so a two-chip module is preferable. The LNA module consists of

two LNA chips, a fixed attenuation pad, transition probes, a printed circuit board (PCB) and a 30-dB coupler terminated with a tapered load. As shown in Fig. 7, the module has a WR-28 input, a coax output, a coax calibration port and a 9-pin bias port. As shown in Fig. 8 of the module interior, input rf signals are fed into a WR-28 waveguide and coupled to a waveguide-to-microstrip transition, followed by two LNA chips separated by a 6-dB attenuation pad. The attenuation pad is used to isolate the two LNAs from each other. The 30-dB waveguide coupler is a multi-aperture design [11] and is used as a calibration port for injecting signals from an external noise source. On the output, rf signals come out of a coax connector via a microstrip-to-coax transition [12]. Bias is supplied to the chips through a PCB with diagnostic and protection circuitry. Chip capacitors are mounted and wire-bonded onto the chassis to bypass signals in the MHz range. The transition probes and attenuation pad are fabricated on alumina substrates using a thin-film process. The dimension of the cavity where chips reside is carefully designed to suppress unwanted waveguide modes. The module measures $5.1 \text{ cm} \times 4.1 \text{ cm} \times 2.0 \text{ cm}$. The module was tested using the N8975A NFM from 26 GHz to 40 GHz. Both noise temperature and associated gain were characterized at room and cryogenic ambient temperatures.

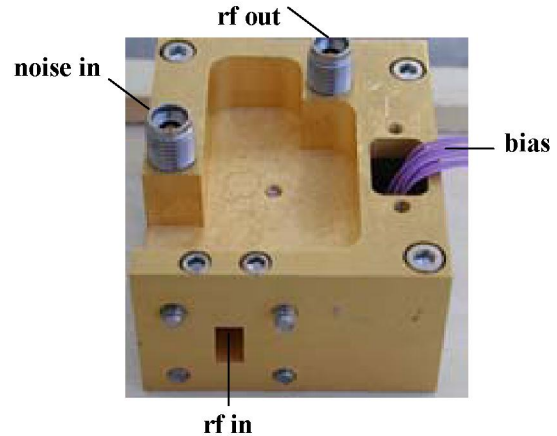


Fig. 7. Photograph of the Ka-band LNA module, WR-28 input, coax output, and an additional coax port for injecting calibration noise signals.

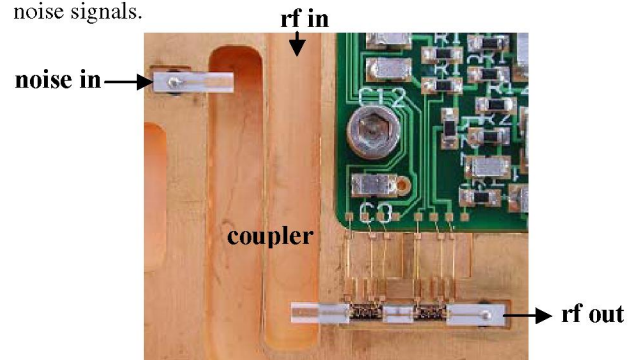


Fig. 8. Photograph of the module interior. Two chips are cascaded with a 6-dB attenuation pad inserted in between the chips.

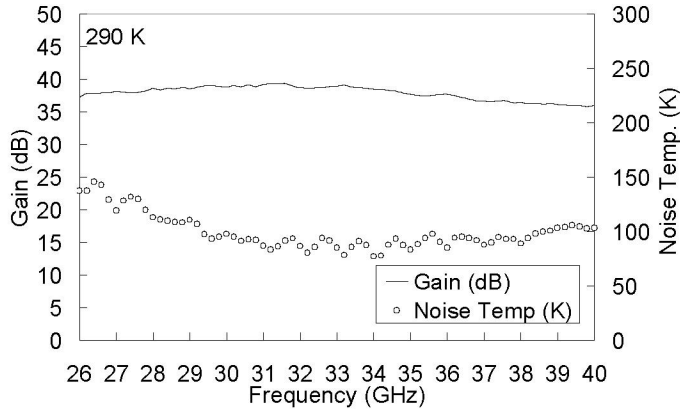


Fig. 9. Measured noise temperature and associated gain of the LNA module, from 26 GHz to 40 GHz, at 290 K.

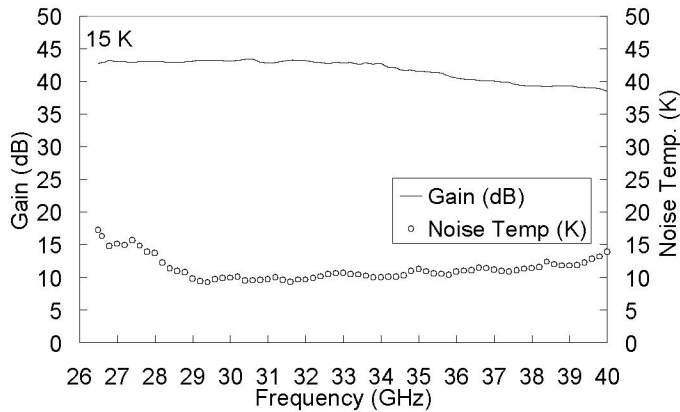


Fig. 10. Measured noise temperature and associated gain of the LNA module, from 26 GHz to 40 GHz, at 15 K.

As shown in Fig. 9, the module at 290 K can achieve an associated gain of 37.6 dB with 1.8 dB flatness for the full Ka band, and an average noise temperature of 99.5 K, equivalent to 1.3 dB noise figure. As the module is cooled to 15 K, average noise temperature is reduced to 11.4 K with 41.0-dB gain and 2.4-dB flatness. At 34 GHz, the module reaches a minimum noise temperature of 9.3 K with 43.2-dB gain.

V. CONCLUSION

A Ka-band MMIC LNA has been developed and achieves high performance over the entire band. The MMIC chip demonstrates flat gain response, low return loss and low noise temperature. By using this MMIC design, a cryogenic LNA module consisting of two chips has been successfully developed. At 300K the module provides 37.6-dB gain and 1.3-dB noise figure and at 15K the module has 43.2 dB gain and 9.3K noise temperature at 34 GHz.

REFERENCES

- [1] J. J. Bautista, J. G. Bowen, J. E. Fernandez, Z. Fujiwara, J. Loreman, S. Petty, J. L. Prater, R. Grundbacher, R. Lai, M. Nishimoto, M. R. Murti, and J. Laskar, "Cryogenic, X-band and Ka-band InP HEMT based LNAs for the Deep Space Network," *Proc. IEEE Aerospace Conf.*, vol. 2, pp. 2/829-2/842, 2001.
- [2] N. Wadefalk, A. Mellberg, I. Angelov, M. E. Barsky, S. Bui, E. Choumas, R. W. Grundbacher, E. L. Kollberg, R. Lai, N. Rorsman, P. Starski, J. Stenarson, D. C. Streit, and H. Zirath, "Cryogenic wide-band ultra-low-noise IF amplifiers operating at ultra-low DC power," *IEEE Trans. Microwave Theory & Tech.*, vol. 51, no. 6, pp. 1705-1711, June 2003.
- [3] S. Weinreb, R. Lai, N. Erickson, T. Gaier, and J. Wielgus, "W-band InP wideband MMIC LNA with 30 K noise temperature," *1999 IEEE MTT-S Int. Microwave Symp. Dig.*, vol. 1, pp. 101-104, June 1999.
- [4] I. Lopez-Fernandez, J. D. G. Puyol, O. J. Homan, and A. B. Cancio, "Low noise cryogenic X-band amplifier using wet-etched, hydrogen passivated InP HEMT devices," *IEEE Microwave and Guided Wave Letters*, vol. 9, pp. 413-415, October 1999.
- [5] N. R. Erickson, R. M. Grosslein, R. B. Erickson, and S. Weinreb, "A cryogenic focal plane array for 85-115 GHz using MMIC preamplifiers," *1999 IEEE MTT-S Int. Microwave Symp. Dig.*, vol. 1, pp. 251-254, June 1999.
- [6] S. Fujimoto, T. Katoh, T. Ishida, T. Oku, Y. Sasaki, T. Ishikawa and Y. Mitsui, "Ka-band ultra low noise MMIC amplifier using pseudomorphic HEMTs," *1997 IEEE MTT-S Int. Microwave Symp. Dig.*, vol. 1, pp. 17-20, June 1997.
- [7] C. Pobanz, M. Matloubian, L. Nguyen, M. Case, M. Hu, M. Lui, C. Hooper, and P. Janke, "A high gain, low power MMIC LNA for Ka-band using InP HEMTs," *1999 IEEE Radio Frequency Integrated Circuits Symp.*, pp. 149-152, June 1999.
- [8] J. B. Hacker, J. Bergman, G. Nagy, G. Sullivan, C. Kadow, H. Lin, A. C. Gossard, M. Rodwell, and B. Brar, "An ultra-low power InAs/AlSb HEMT Ka-band low-noise amplifier," *2004 IEEE Microwave And Wireless Components Letters*, vol. 14, no. 4, pp. 156-158, April 2004.
- [9] N. Rorsman, M. Garcia, C. Karlsson, and H. Zirath, "Accurate small-signal modeling of HFETs for millimeter-wave applications," *IEEE Trans. Microwave Theory & Tech.*, vol. 44, pp. 432-437, March 1996.
- [10] M. W. Pospieszalski, "Modeling of noise parameters of MESFETs and MODFETs and their frequency and temperature dependence," *IEEE Trans. Microwave Theory & Tech.*, vol. 37, pp. 1340-1350, September 1989.
- [11] N. Erickson, "High performance dual directional couplers for near-mm wavelengths," *2001 IEEE Microwave And Wireless Components Letters*, vol. 11, no. 5, pp. 205-207, May 2001.
- [12] M. Morgan and S. Weinreb, "A millimeter-wave perpendicular coax-to-microstrip transition," *2002 IEEE MTT-S Int. Microwave Symp. Dig.*, pp. 817-820, Seattle, WA, June 2002.